

Electronic Supplementary Information (ESI) for

Topological Entrapment of Macromolecules During the Formation of Metal–Organic Frameworks

Nagi Mizutani, Nobuhiko Hosono,* and Takashi Uemura*

Table of Contents

1. General	1
2. Materials	2
3. Methods	3
4. Molecular weight dependence of the encapsulation efficiency and retention behavior of PEG	4
5. Supporting Table	5
6. Supporting Figures	6
7. Supporting References	23

1. General

¹H and ¹³C nuclear magnetic resonance (NMR) spectra were recorded using a JEOL model ECS-400 spectrometer (400 MHz and 100 MHz, respectively) and a Bruker Avance III HD (500 MHz and 125 MHz, respectively) spectrometer equipped with a PABBO probe. X-ray powder diffraction (XRPD) data were recorded on a Rigaku model SmartLab X-ray diffractometer using Cu K α radiation. Differential scanning calorimetry (DSC) was carried out using Hitachi High-Tech Science Corporation model DSC-6020 and DSC7020 at the heating rate of 10 K/min under continuous nitrogen flow. Matrix-assisted laser desorption/ionization time-of-flight mass (MALDI-TOF MS) spectra were recorded on an AB Sciex TOF/TOF 5800 using α -cyano-4-hydroxycinnamic acid (CHCA) as the matrix. Size-exclusion chromatography (SEC) with tetrahydrofuran (THF) eluent was performed using two polystyrene gel columns in series (Shodex LF-804) at 40 °C on a Shodex model GPC-101 system equipped with refractive index (RI) and UV detectors. The flow rate was 1.0 mL/min. SEC with DMF (10 mM LiBr) eluent was performed using two polystyrene gel columns in series (Shodex KD-806M) at 60 °C on a Shodex model GPC-101 system equipped with RI and UV detectors. The flow rate was 1.0 mL/min. Scanning electron microscopy (SEM) was performed using a Hitachi model SU-5000 at an accelerating voltage of 20 kV. Samples were deposited on a conducting carbon tape attached on a SEM sample holder, then coated with platinum. Gas adsorption measurements were performed using MicrotracBEL model BELSORP-mini. Particle size distribution analysis was carried out using HORIBA model laser scattering particle size analyzer Partica LA-950. The samples were dispersed in acetone at 25 °C. IR spectra were recorded by a JASCO FT/IR-4200. Solid-state NMR measurement was performed on a 9.4 T Bruker solid-state NMR instrument with an Avance III 400 MHz spectrometer and a double resonance 4 mm magic angle spinning probe with a spinning rate of 12 kHz at 25 °C.

2. Materials

All reagents and chemicals used in this study were purchased from FUJIFILM Wako Pure Chemicals and TCI Chemicals, unless otherwise noted. Deuterated solvents for NMR spectroscopy were purchased from Cambridge Isotope Laboratories. Polyethylene glycols (PEGs) with molecular weights (MWs) of 910 g/mol (1k), 1,960 g/mol (PEG, 2k), 200 kg/mol (200k) were purchased from Sigma Aldrich, and 21,100 (20k) g/mol was purchased from Alfa Aesar. All PEGs were used without further purification.

2.1. Synthesis of 1. $[\text{Zn}_2(\text{ndc})_2\text{ted}]_n$ (**1**) (ndc = 1,4-naphthalenedicarboxylate, ted = triethylenediamine) was synthesized according to the previously reported procedure with a slight modification.¹ $\text{Zn}(\text{NO}_3)_2 \cdot 4\text{H}_2\text{O}$ (0.26 g, 1.0 mmol), H_2ndc (0.22 g, 1.0 mmol) and ted (0.056 g, 0.50 mmol), were placed in a glass vessel. To the vessel, *N,N*-dimethylformamide (DMF) (1 mL) was added. The vessel was sealed and heated at 120 °C for 24 h without stirring. The crystals were washed with acetonitrile (ACN, 20 mL) for 6 times then dried under vacuum for 18 h, affording **1** (0.31 g) with the particle diameter of $31.6 \pm 22.1 \mu\text{m}$ (Fig. S7 and S8).

To have **1** with better particle size control, we performed the same reaction with stirring the mixture and using different concentration conditions.¹ **1** with the particle diameter of $28.6 \pm 22.4 \mu\text{m}$ was obtained, which was used as the host for the direct insertion method providing **1**⊃PEG_{ins}.

2.2. Synthesis of poly(methyl methacrylate) (PMMA). PMMA was synthesized by reversible addition–fragmentation chain transfer (RAFT) polymerization. Methyl methacrylate (MMA) was purified by vacuum distillation prior to use. MMA (44.6 mmol, 4.77 mL), 2-cyano-2-propyl benzodithioate (CPBdT, 0.446 mmol, 98.7 mg), and 2,2'-azobis(isobutyronitrile) (AIBN) (0.0889 mmol, 14.6 mg) were dissolved in toluene (4.77 mL). After bubbling nitrogen for 5 min at 0 °C, the mixture was heated at 70 °C for 21.5 h. After cooling down to 25 °C, the mixture was poured into an excess amount of hexane. The precipitate was collected by filtration and dissolved again in dichloromethane. This reprecipitation process was repeated for three times. The product was dried under vacuum at 25 °C for 19.5 h, affording PMMA (4.1 g). MW data is given in Table S1.

¹H NMR (500 MHz, CDCl₃): δ (ppm) 7.89 (ArH of CPBdT, br), 7.52 (ArH of CPBdT, br), 7.36 (ArH of CPBdT, br), 3.70-3.50 (-OCH₃, br), 2.00-1.71 (-CH₂-, br), 1.10-0.95 (-CCH₃, br), 0.91-0.75 (-CCH₃, br).

2.3. Synthesis of poly(4-vinylpyridine) (PVP). PVP was synthesized by RAFT polymerization. 4-Vinylpyridine (VP) was purified by vacuum distillation prior to use. VP (47.5 mmol, 5.05 mL), CPBdT (0.474 mmol, 105 mg), and AIBN (0.0969 mmol, 15.9 mg) were dissolved in DMF (5.05 mL) and bubbled with nitrogen. The mixture was heated and stirred at 70 °C for 6.5 h. After cooling down to 25 °C, the mixture was poured into an excess amount of diethyl ether. The precipitate was collected by filtration and dissolved again in dichloromethane. This reprecipitation process was repeated for three times. The product was dried under vacuum at 25 °C for 19.5 h, affording PVP (2.0 g). MW is given in Table S1.

¹H NMR (500 MHz, CDCl₃): δ (ppm) 8.65-8.07 (ArH, PVP), 7.84 (ArH of CPBdT, br), 7.54 (ArH of CPBdT, br), 7.36 (ArH of CPBdT, br), 6.86-6.02 (ArH, PVP), 2.39-1.23 (-CH₂-, -CCH- br).

2.4. Synthesis of CPEG. CPEG was synthesized according to the previously reported procedure with a slight modification.² Under a nitrogen atmosphere, finely powdered KOH (2.2 g) was dispersed in anhydrous THF/heptane (75/25, 100 mL). To the KOH dispersion, anhydrous THF solution (100 mL) of PEG (MW 1,960, 3.33 mmol, 6.66 g) and tosyl chloride (3.33 mmol, 635 mg) was added dropwise at 40 °C for 48 h, then the mixture was further stirred at 40 °C for 24 h. After cooling down to 25 °C, the mixture was filtered, and all solvents were evaporated under a reduced pressure. The solid residue was dissolved in water and neutralized by adding HCl solution. The aqueous solution was extracted with dichloromethane and the organic phase was evaporated to dryness. The crude product thus obtained was dried in vacuo for 18 h at 25 °C.

To have authentic CPEG for use in **1**+CPEG reaction, isolation of cyclic PEG from the crude product was carried out by following procedure described in the literature.³ Activated **1** (22.4 g) was dispersed in ACN solution (100 mL) of the crude product (5.60 g). Then, the solvent was slowly removed under a reduced pressure. Once all the solvent was evacuated, the mixture was annealed for 18 h at 120 °C under dynamic vacuum while linear PEGs

were selectively adsorbed in **1**. Successively, ethanol (100 mL) was added to the mixture and the sample was washed for 30 s by shaking at 25 °C. Then, the solid was filtered off and the filtrate was evaporated to dryness. Powdery product was dissolved in dichloromethane (10 mL) then precipitated from hexane (1 L). The precipitate was collected and dried in vacuo for 18 h at 25 °C, affording CPEG (2.36 g). SEC data is given in Fig. S13.

¹H NMR (500 MHz, CDCl₃): δ (ppm) 3.64 (-CH₂-).

¹³C NMR (100 MHz, CDCl₃): δ (ppm) 70.6 (-CH₂-).

3. Methods

3.1. *In-situ* MOF formation with PMMA (1+PMMA). The reaction at 120 °C is described in detail. Zn(NO₃)₂·4H₂O (0.26 g, 1.0 mmol), H₂ndc(0.22 g, 1.0 mmol), ted (0.056 g, 0.50 mmol), DMF (1 mL), and PMMA (50 mg) were mixed and heated at 120 °C for 24 h without stirring. After cooling down to 25 °C, the crystalline product was collected by filtration. To remove the excess PMMA existing on the surface of crystals, the product was washed by solvents as follows. The product was dispersed in ACN (20 mL) then collected by centrifugation. The product was washed again by using chloroform (20 mL) as the solvent. The product was dried in vacuo for 18 h at 25 °C and subjected to the characterization (Yield: 0.31 g).

3.2. *In-situ* MOF formation with PVP (1+PVP). The reaction at 120 °C is described in detail. Zn(NO₃)₂·4H₂O (0.26 g, 1.0 mmol), H₂ndc(0.22 g, 1.0 mmol), ted (0.056 g, 0.50 mmol), DMF (1 mL), and PVP (50 mg) were mixed and heated at 120 °C for 24 h without stirring. After cooling down to 25 °C, the crystalline product was collected by filtration. To remove the excess PVP existing on the surface of crystals, the product was washed by solvents as follows. The product was dispersed in ACN (20 mL) then collected by centrifugation. The product was washed again by using chloroform (20 mL) as the solvent. The product was dried in vacuo for 18 h at 25 °C and subjected to the characterization (Yield: 0.10 g).

3.3. *In-situ* MOF formation with PEG (1+PEG). The reaction at 120 °C with PEG (MW: 1,960 g/mol, 50 mg) is described in detail. Zn(NO₃)₂·4H₂O (0.26 g, 1.0 mmol), H₂ndc (0.22 g, 1.0 mmol), ted (0.056 g, 0.50 mmol), DMF (1 mL), and PEG (MW: 1,960 g/mol) (50 mg) were mixed and heated at 120 °C for 24 h. After cooling down to 25 °C, the crystalline product was collected by filtration. To remove the excess PEG existing on the surface of crystals, the product was washed by a solvent as follows. The product was dispersed in ACN (20 mL) then collected by centrifugation. This procedure was repeated for 6 times. The product was dried in vacuo for 18 h at 25 °C and subjected to the characterization (Yield: 0.33 g).

3.4. Direct insertion of PEG into **1 (preparation of 1▷PEG_{ins}).** 1▷PEG_{ins} was prepared according to the previously reported direct insertion method.⁴ The pre-activated **1** (200 mg) was dispersed in an ACN solution (1 mL) of PEG (MW: 1,960 g/mol) (60 mg). Then, the solvent was slowly removed under a reduced pressure. Once all the solvent was evacuated, the mixture was annealed for 18 h at 120 °C under dynamic vacuum. To remove the excess PEG existing on the surface of **1**, the resultant powdery mixture was washed by a solvent as follows. The product was dispersed in ACN (20 mL) then collected by centrifugation. This procedure was repeated for 6 times. The product was dried in vacuo at 25 °C for 18 h, affording 1▷PEG_{ins}.

3.5. Procedure of the repetitive washing experiment. Typically, 1▷PEG composite (20 mg) was immersed in THF (10 mL) and subjected to sonication for 10 min at 25 °C. The washed composite was collected by filtration. One portion of the washed composite was taken and analyzed by ¹H NMR to quantify the amount of PEG remaining inside **1**. This procedure was repeated for three times.

3.6. Procedure of the cyclic/linear PEG separation by *in-situ* encapsulation method. Zn(NO₃)₂·4H₂O (0.26 g, 1.0 mmol), H₂ndc(0.22 g, 1.0 mmol), ted (0.22 g, 2.0 mmol), DMF (1 mL), and the crude product of PEG cyclization reaction (1.5 g, see Section 2.4) were mixed and left to stand at 25 °C for 24 h. Crystalline product was obtained. The product (60 mg) was dispersed in dichloromethane (60 mL) and washed by sonication for 18 h. The

product was further washed with stirring in dichloromethane (30 mL) for 10 min, then collected by filtration. This washing process was repeated for three times. To digest the host **1** for recovering the PEG trapped, the composite was added to ethylenediamine-*N,N,N',N'*-tetraacetic acid tetrasodium salt (EDTA·4Na) aqueous solution (excess amount). The aqueous solution was extracted with chloroform and the organic phase was evaporated to dryness, leaving only cyclic PEG that is successfully isolated from linear byproducts.

3.7. Quantification of the amount of PEG inside 1. **1**⊃PEG was dissolved in DMSO-*d*₆/35%DCl in D₂O (9/1, v/v) and analyzed by ¹H NMR. The PEG/MOF mass ratio (g/g) was calculated according to the following formula,

$$\text{Mass of PEG inside } \mathbf{1} \text{ per unit mass} = \frac{x \times (\text{MW of PEG})}{(\text{Number of protons in a PEG chain}) \times (\text{MW of } [\text{Zn}_2(\text{ndc})_2(\text{ted})])}$$

, where *x* is the integral value of the proton peak corresponding to the PEG main chain (δ 3.4 ppm). The sum of the integral values of the proton peaks corresponding to ndc (δ 7.63, 8.01, 8.64 ppm) is normalized to be 12.

4. Molecular weight dependence of the encapsulation efficiency and retention behavior of PEG

The molecular weight (MW) dependence of the polymer encapsulation was investigated using PEGs with different MWs, *M*_n = 910 g/mol, 1,960 g/mol, 21,100 g/mol, 200 kg/mol, and 2,000 kg/mol (hereafter denoted as 1k, 2k, 20k, 200k, and 2M, respectively, Table S1), as additives (1.0 g/mL) in the preparation of **1** at 120 °C. The representative procedure (see Section 3.3) was used. PXRD data of the products suggested that all reactions successfully provided high-quality **1** crystals (Figure S11).

The PEG loading amount of each composite was determined by ¹H NMR analysis on the acid-digested sample (Figure S12a). The composites with relatively short PEGs (1k to 20k) were loaded at ~30 wt%, which corresponds to the maximum loading capacity, whereas longer PEGs (200k and 2M) were loaded at 5–10 wt% (Figure S12a). This trend could be attributed to the volume exclusion effect of the polymers, which possibly causes the segregation of polymer chains and MOF components in the reaction mixture.

We also investigated MW-dependence of PEG retention in **1**. When the composites synthesized with 1k, 2k, and 20k PEGs were washed three times with THF (Figure S12b), the composite with 1k PEG exhibited the fastest release of PEG whereas that with 20k showed the slowest release. This trend is reasonable considering that the interaction between the MOF and PEG becomes more pronounced as the polymer MW increases.

5. Supporting Table

Table S1. Molecular weights of polymers used in this study.

Code	M_n	M_w	M_w/M_n
PMMA ^{a)}	7,060	9,220	1.31
PVP ^{a)}	6,940	10,640	1.53
1k ^{b)}	910	960	1.05
PEG (2k) ^{b)}	1,960	2,030	1.04
20k ^{b)}	21,100	23,600	1.11
200k	N/A ^{c)}	N/A ^{c)}	N/A ^{c)}
2M	N/A ^{c)}	N/A ^{c)}	N/A ^{c)}

^{a)}Determined by SEC calibrated with polystyrene standards. ^{b)}Determined by SEC calibrated with PEG standards.

^{c)}N/A because of size exclusion limit of the column. Thus, the MW information given by the supplier was used as nominal MW for these samples.

6. Supporting Figures

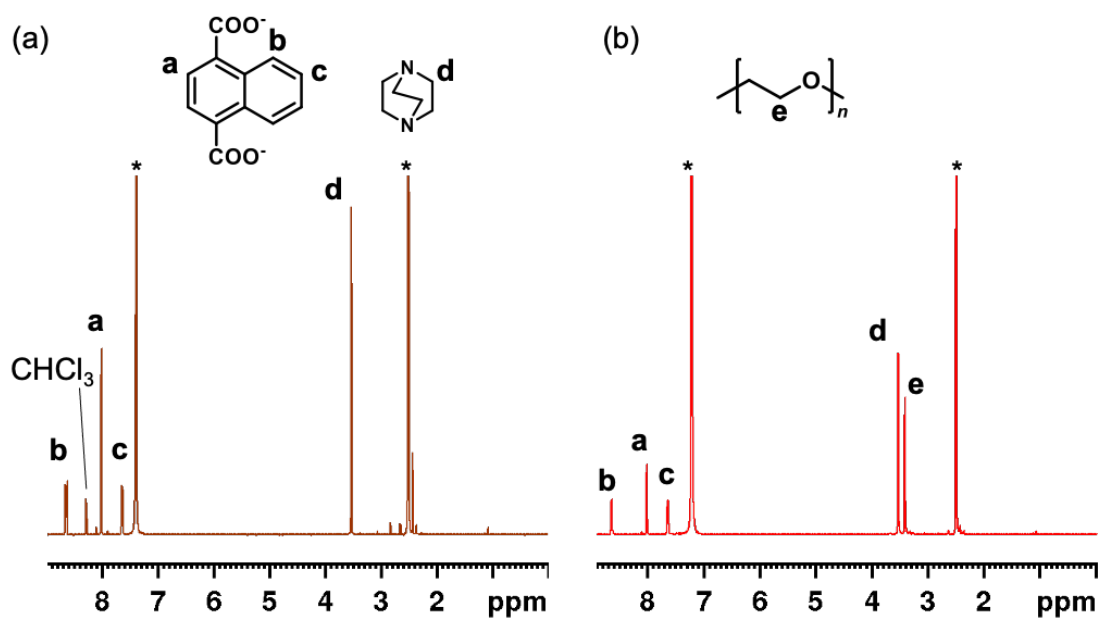


Figure S1. ^1H NMR spectra of (a) the product of 1+PMMA and (b) 1+PEG, digested in an acidified deuterated solvent (DMSO- d_6 /DCl, 9/1, v/v). 1+PMMA sample showed no proton signal corresponding to PMMA chain whereas 1+PEG sample showed the PEG signal as peak e. Asterisks denote the signals from residual protons in DCl and DMSO- d_6 .

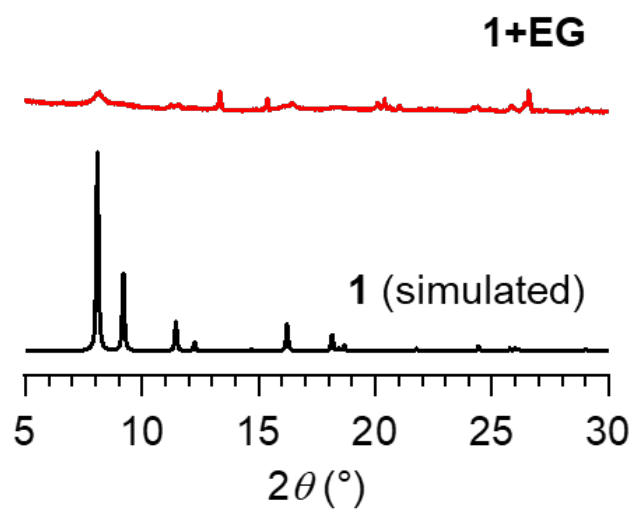


Figure S2. PXRD data of the product obtained from the **1** formation reactions at 25 °C in the presence of ethylene glycol (**1+EG**). Black line denotes the simulated PXRD pattern of **1** single crystal.

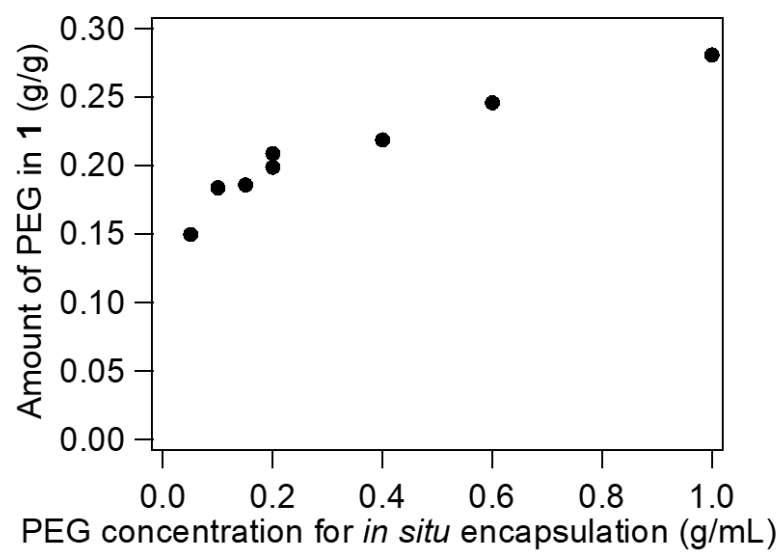


Figure S3. Relationship between the encapsulated PEG amount in **1** and PEG solution concentration used for the *in-situ* encapsulation reaction.

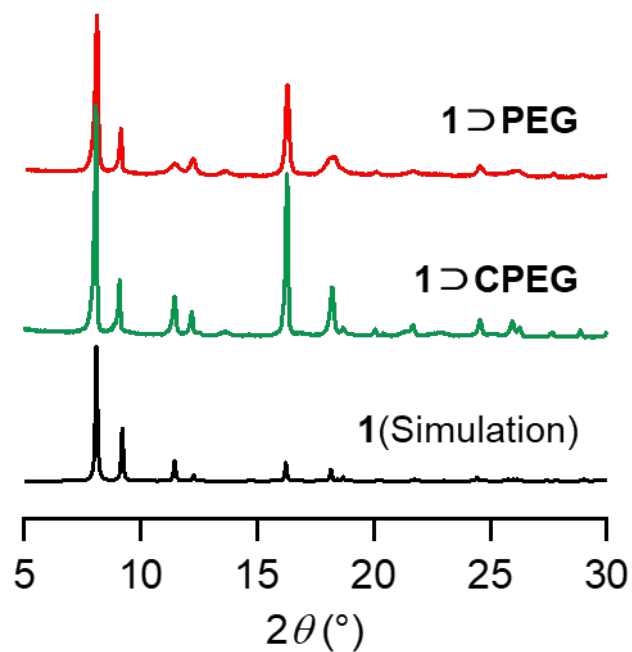


Figure S4. PXRD data of the **1/PEG** composites, (red) **1 \supset PEG** and (green) **1 \supset CPEG**, obtained from **1** formation reactions at 120 °C in the presence of respective PEGs (1.0 g/mL). Black line denotes the simulated PXRD pattern of **1** single crystal.

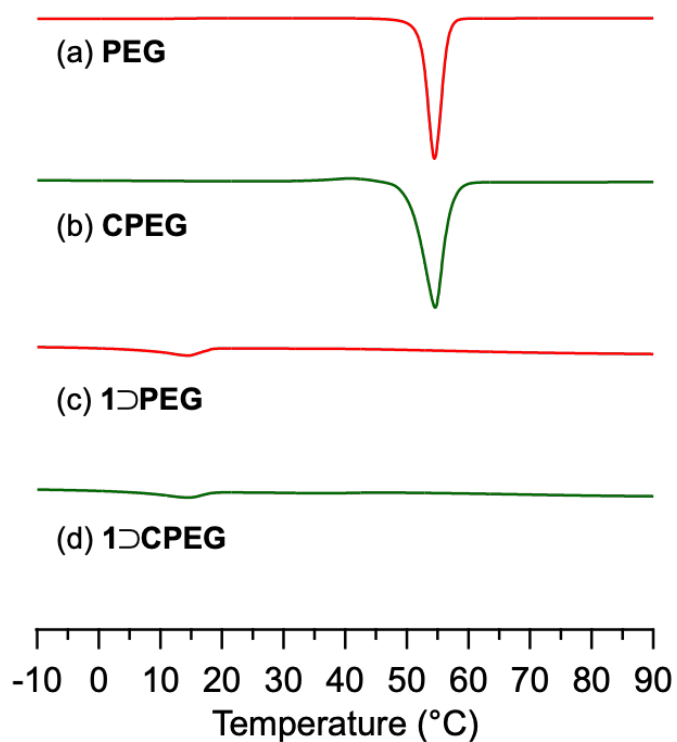


Figure S5. DSC curves on the second heating cycle for (a) pristine PEG and (b) CPEG, and **1**/PEG composites, (c) **1**⊃PEG and (d) **1**⊃CPEG, obtained from the **1** formation reactions at 120 °C in the presence of respective PEGs (1.0 g/mL). The shift of the melting peak (~54 °C) to lower temperature (~14 °C) indicates entire encapsulation of PEG in **1**. The disappearance of the original melting peak ensures that no PEG is present outside of the **1** crystals.

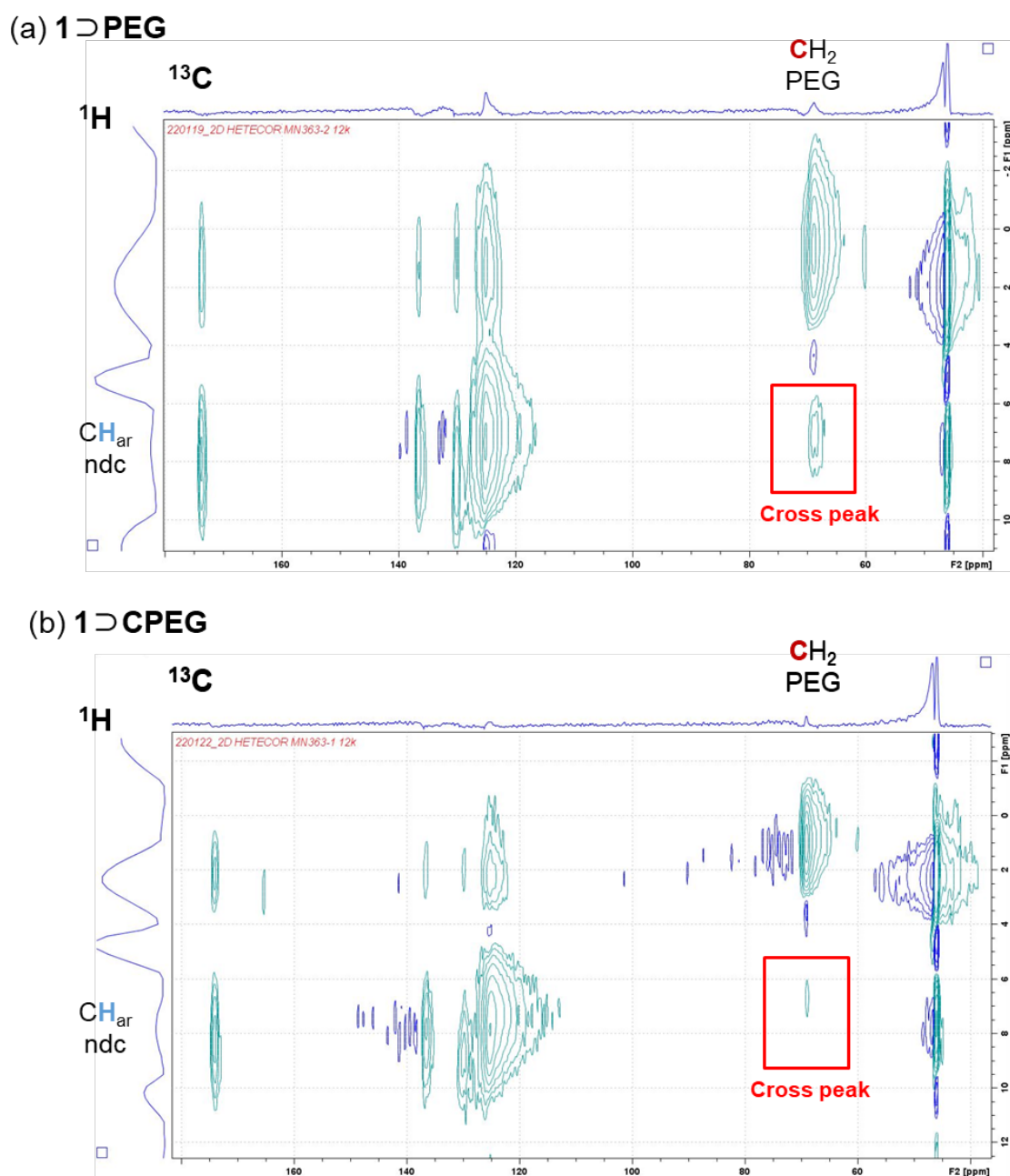


Figure S6. Solid-state HETCOR 2D NMR spectra of (a) **1**⊃PEG and (b) **1**⊃CPEG composites. Cross peaks between the carbon of PEG main chain and the proton of ndc ligand were observed. This indicates the presence of host-guest interaction between **1** framework and PEG chain.

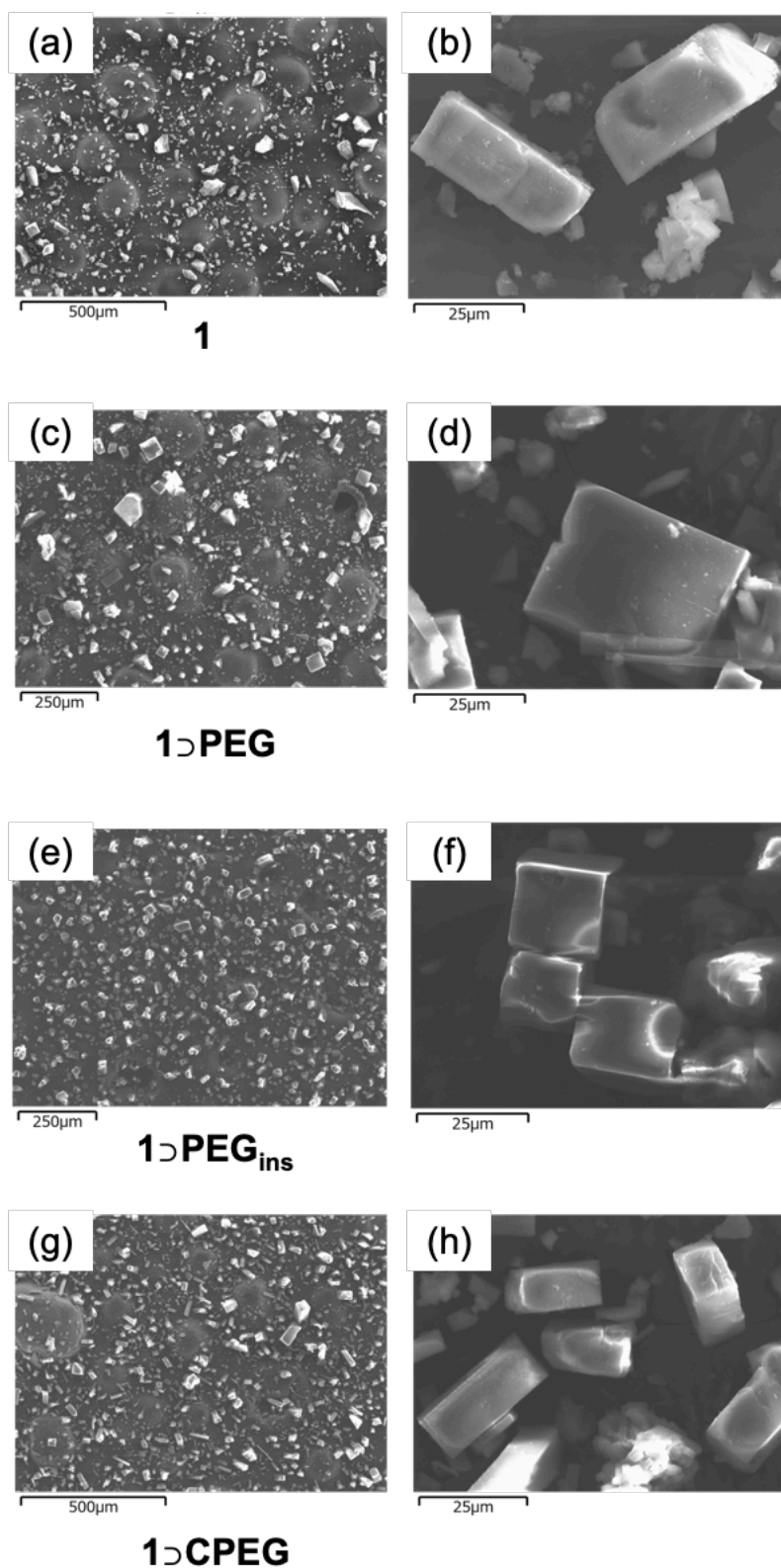


Figure S7. SEM images of (a, b) **1**, (c, d) **1⊃PEG**, (e, f) **1⊃PEG_{ins}**, and (g, h) **1⊃CPEG**. No obvious morphology difference was observed.

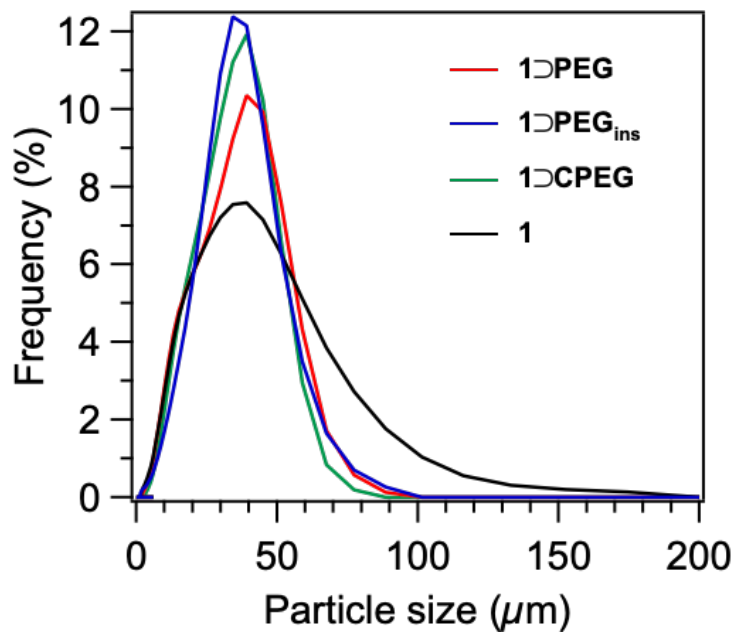


Figure S8. Particle size distribution data of (red) **1DPEG** ($28.1 \pm 15.0 \mu\text{m}$), (blue) **1DPEG_{ins}** ($29.2 \pm 14.0 \mu\text{m}$), (green) **1DCPEG**, ($28.1 \pm 13.0 \mu\text{m}$) and (black) **1** synthesized without polymer additive ($31.6 \pm 22.1 \mu\text{m}$). No significant size difference was observed although **1** without polymer additive showed rather wider size distribution with contamination of large particles. It should be noted that the host **1** crystals used for **1DPEG_{ins}** was synthesized in the different batch with controlling particle size to make the size range and distribution comparable to **1DPEG**.

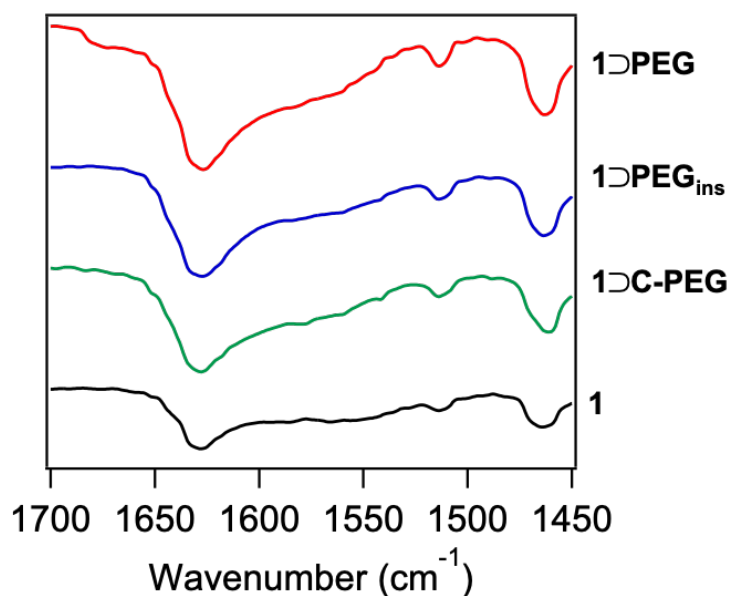


Figure S9. FT-IR spectra of **1@PEG** composites. (red) **1@PEG** and (green) **1@CPEG** synthesized at 120 °C in the presence of respective PEG (1.0 g/mL). (blue) **1@PEG_{ins}** prepared by the post-synthetic insertion method. Black line denotes the FT-IR spectrum of **1** with controlled particle size (i.e. host for **1@PEG_{ins}**). The absorption peaks in 1600-1650 cm^{-1} and 1550-1600 cm^{-1} are attributed to asymmetric stretching vibration of carboxylate binding to zinc ions through bidentate coordination and that of uncoordinated carboxylate, respectively.⁵ The presence of latter peak (1550-1600 cm^{-1}) can be used as a measure of defect structure in the MOF crystal. For all samples, the latter peak is weaker than the former peak (1600-1650 cm^{-1}), indicating all crystals have less defects in the coordination network.

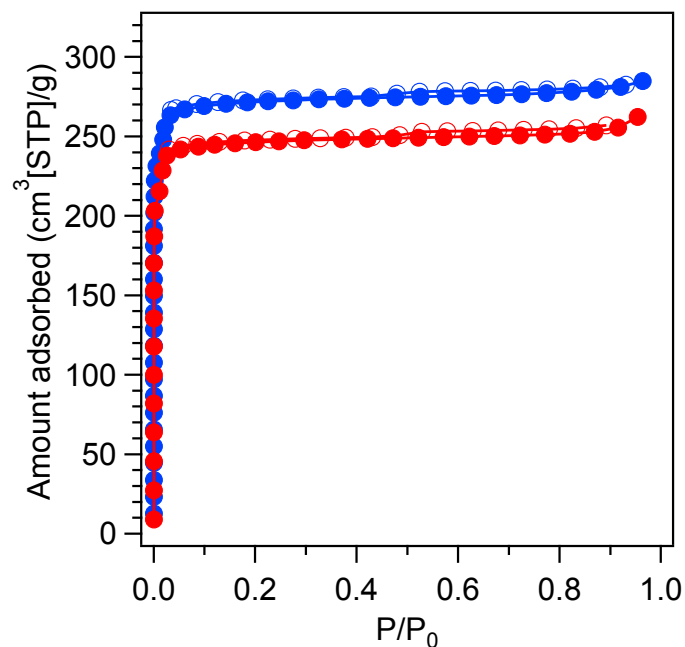


Figure S10. N₂ adsorption isotherms of (blue) **1** without polymer additive and (red) **1**+PEG after the rigorous washing treatment. (filled circle) adsorption isotherm and (open circle) desorption isotherm at 77 K. The total pore volume of **1** without polymer additive was calculated to be 0.44 mL/g at P/P₀ = 0.96, which is in agreement with the reported value.^{1b,6} The total pore volume of the **1**+PEG sample after the washing treatment was calculated to be 0.41 mL/g at P/P₀ = 0.95. This is slightly less than the pore volume of **1** (0.44 mL/g) due to the presence of residual PEG chain in the pore (3.4 wt%).

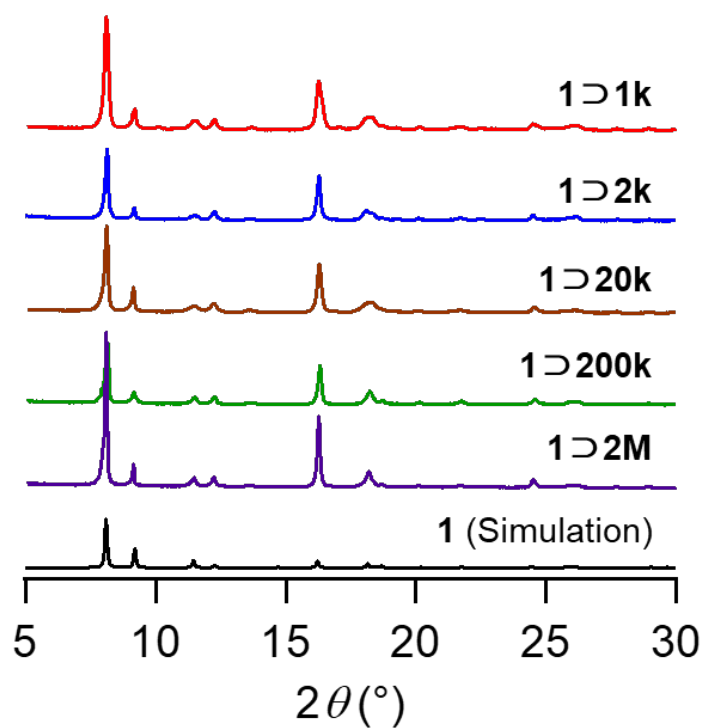


Figure S11. PXRD data of the 1/PEG composites obtained using PEGs with various MWs, 1k, 2k, 20k, 200k, and 2M (120 °C, 1.0 g/mL). (red) 1⊃1k, (blue) 1⊃2k, (brown) 1⊃20k, (green) 1⊃200k, and (purple) 1⊃2M. Black line denotes the simulated PXRD pattern of 1 single crystal.

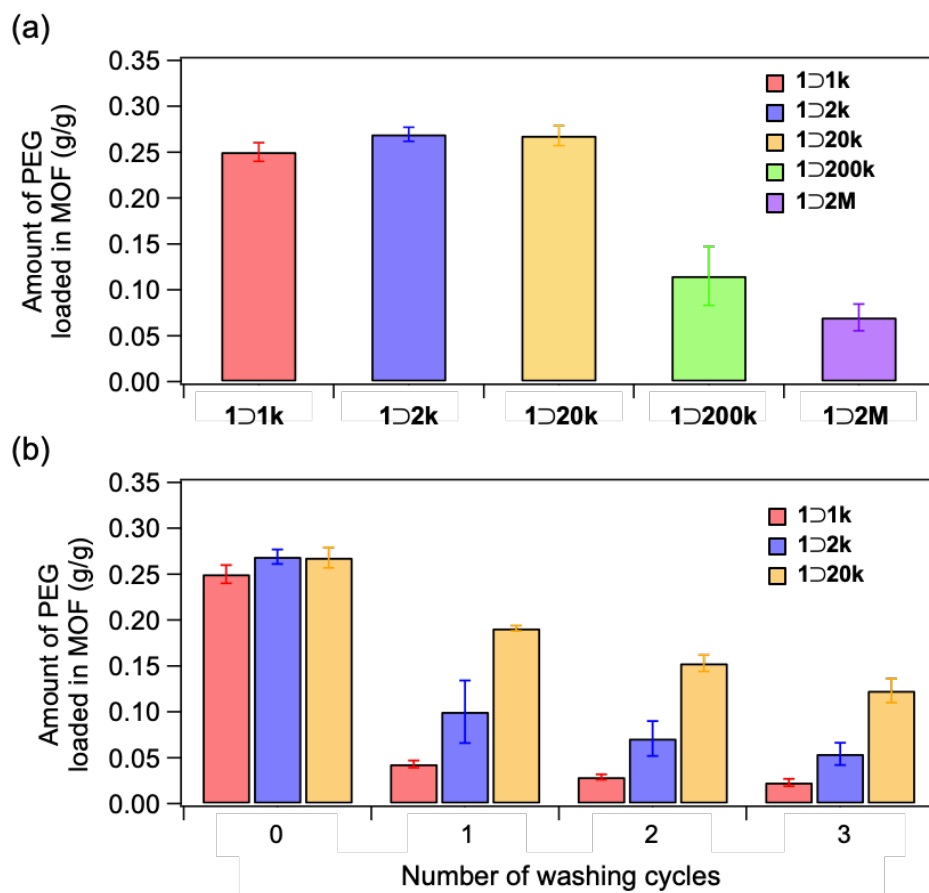


Figure S12. Molecular weight dependence of (a) the amount of PEG encapsulated in **1** and (b) the amount of residual PEG in **1** after given number of washing cycles. (red) **1D1k**, (blue) **1D2k**, (yellow) **1D20k**, (green) **1D200k**, and (purple) **1D2M**. Error bars indicate standard errors ($N = 4$ for **1D200k**, $N = 3$ for others).

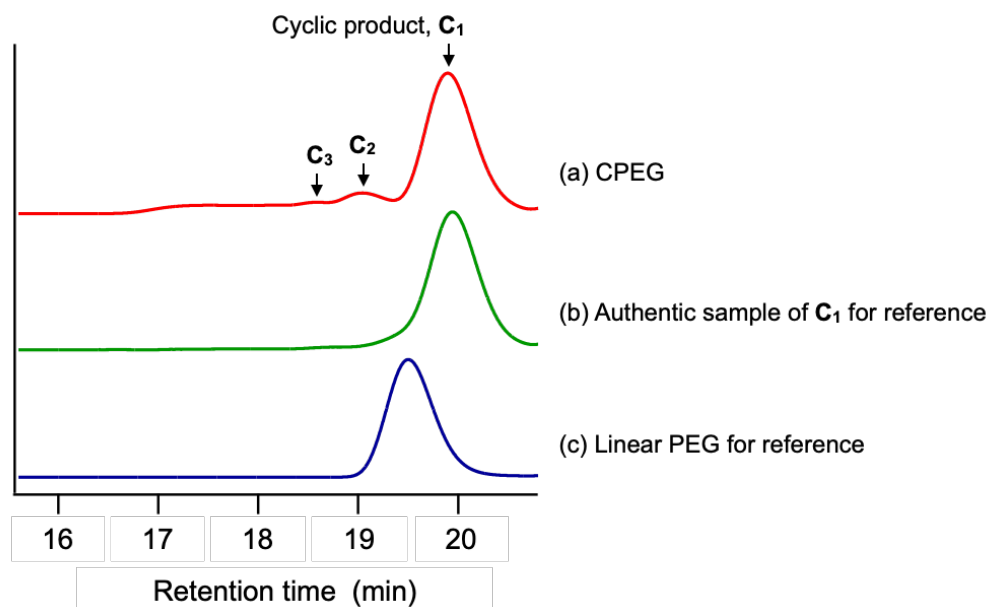


Figure S13. SEC chromatograms of (a) CPEG, (b) an authentic sample of mono-cyclized product (C_1) for reference, and (c) linear PEG ($M_n = 1,960$ g/mol) that was used for the CPEG synthesis. CPEG contains cyclization products formed intramolecular (C_1) and intermolecular coupling of multiple chains (C_n , $n = 2, 3 \dots$).³ The authentic sample of C_1 was synthesized and carefully purified according to the previously reported procedure.² The elution peak position of C_1 of CPEG is identical to that of the authentic sample, indicating the successful synthesis of CPEG. There is no elution peak corresponding to the linear PEG (starting material) in (a). This ensures high cyclic purity of CPEG.

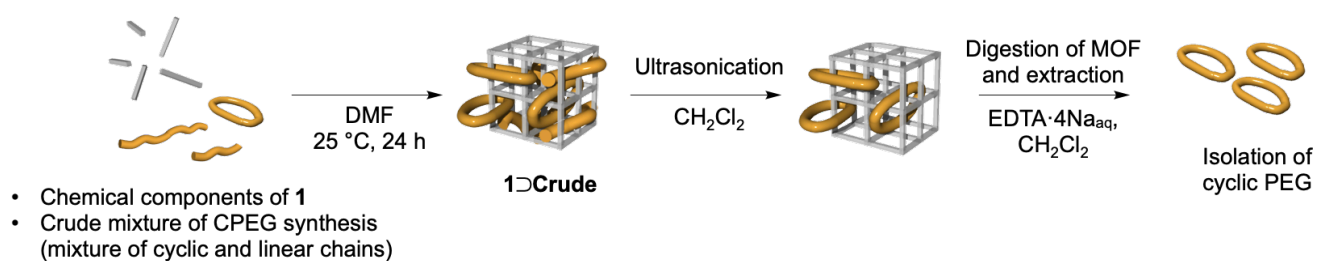


Figure S14. Scheme of the cyclic/linear PEG separation by *in-situ* encapsulation method.

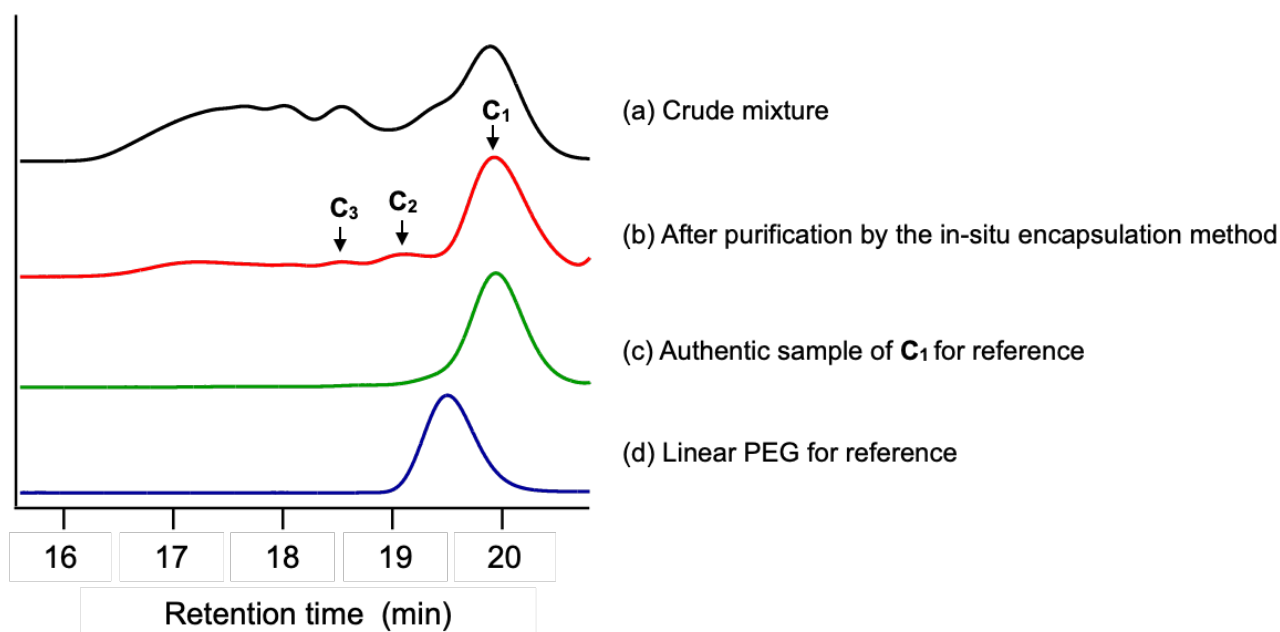


Figure S15. SEC chromatograms of (a) the crude mixture of CPEG synthesis, (b) the product after purification of the crude material by the *in-situ* encapsulation method, (c) the authentic sample of C₁ for reference, and (d) linear PEG ($M_n = 1,960$ g/mol) that was used for the CPEG synthesis. The crude mixture contains both cyclic and linear species. After the purification by the *in-situ* encapsulation method, the elution peak corresponding to the linear PEG disappeared, indicating the successful isolation of cyclic species from the mixture.³

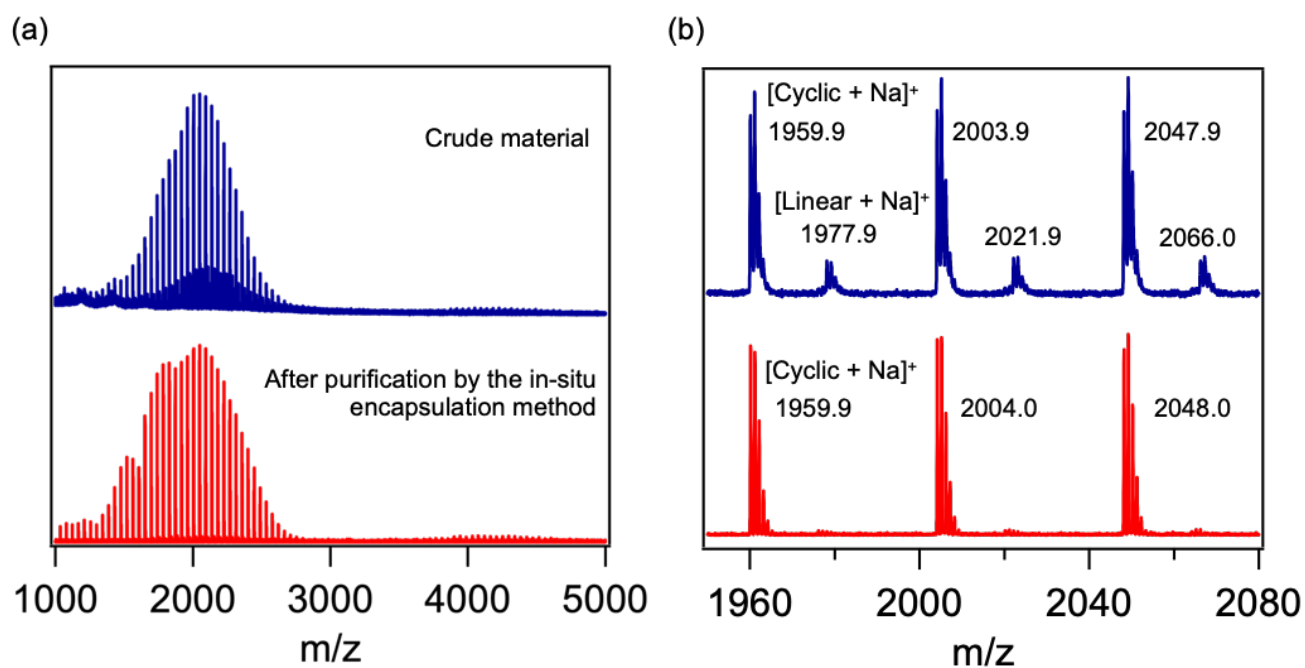


Figure S16. (a) MALDI-TOF mass spectra of (blue) the crude mixture of CPEG synthesis and (red) the product after purification of the crude mixture by the *in-situ* encapsulation method. (b) A magnified view (1950-2080 m/z) of the panel a. CHCA was used as the matrix. While the crude mixture shows signals of both linear and cyclic species, the product after purification by the *in-situ* encapsulation method shows only the signals of cyclic species, $[(\text{CH}_2\text{CH}_2\text{O}) \times n + \text{Na}]^+$ (n denotes degree of polymerization).³

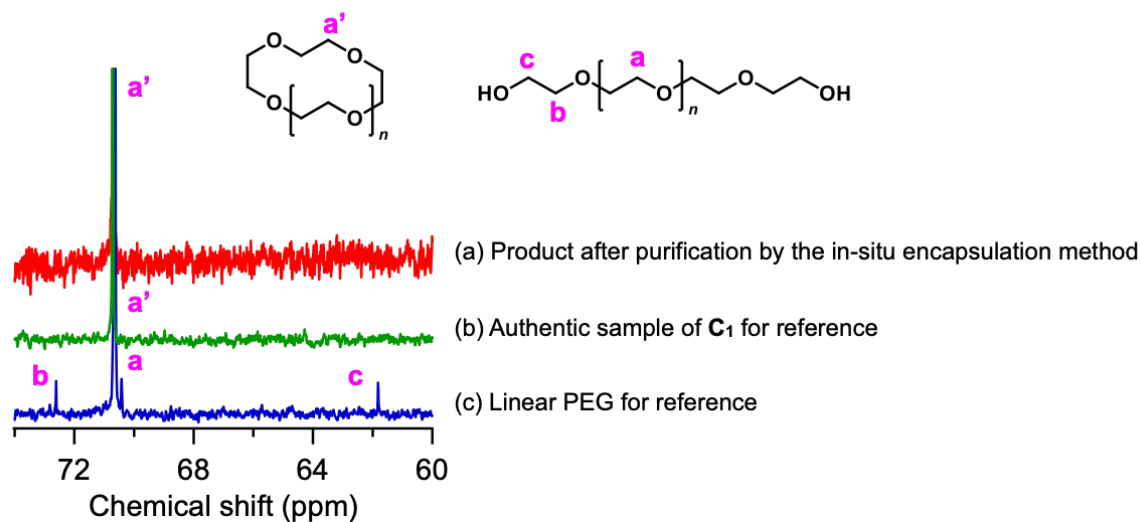


Figure S17. ^{13}C NMR spectra of (a) the product after purification of the crude mixture by the *in-situ* encapsulation method, (b) the authentic sample of C_1 for reference, and (c) linear PEG ($M_n = 1,960$ g/mol) that was used for the CPEG synthesis. Peak a corresponds to the signal from the main chain carbon (a' denotes that of cyclic PEG). Peak b and c correspond to the terminal carbons of the linear PEG. The product after purification by the *in-situ* encapsulation method shows complete absence of peaks b and c, suggesting the successful isolation of cyclic species from the crude mixture.³

7. Supporting References

- 1 (a) N. Mizutani, N. Hosono, B. L. Ouay, T. Kitao, R. Matsuura, T. Kubo, T. Uemura, *J. Am. Chem. Soc.* **2020**, *142*, 3701–3705. (b) H. Chun, D. N. Dybtsev, H. Kim, K. Kim, *Chem. Eur. J.* 2005, **11**, 3521–3529.
- 2 J. Cooke, K. Viras, G.-E. Yu, T. Sun, T. Yonemitsu, A. J. Ryan, C. Price, C. Booth, *Macromolecules* 1998, **31**, 3030–3039.
- 3 T. Sawayama, Y. Wang, T. Watanabe, M. Takayanagi, T. Yamamoto, N. Hosono, T. Uemura, *Angew. Chem. Int. Ed.* 2021, **60**, 11830–11834.
- 4 B. Le Ouay, C. Watanabe, S. Mochizuki, M. Takayanagi, M. Nagaoka, T. Kitao, T. Uemura, *Nat. Commun.*, 2018, **9**, 3635.
- 5 (a) V. Zeleňák, Z. Vargová, K. Györyová, *Spectrochim. Acta A* 2007, **66**, 262–272. (b) K. Tan, N. Nijem, P. Canepa, Q. Gong, J. Li, T. Thonhauser, Y. J. Chabal, *Chem. Mater.* 2012, **24**, 3153–3167. (c) Z. Su, Y.-R. Miao, G. Zhang, J. T. Miller, K. S. Suslick, *Chem. Sci.* 2017, **8**, 8004–8011.
- 6 K. Kioka, N. Mizutani, N. Hosono, T. Uemura, *ACS Nano* 2022, **16**, 6771–6780.